ADVANCED MATERIALS
www.advmat.de

Cardiomyocytes-Actuated *Morpho* Butterfly Wings

*Zhuoyue Chen, Fanfan Fu, Yunru Yu, Huan Wang, Yixuan Shang, and Yuanjin Zhao**

***Morpho* butterflies are famous for their wings' brilliant structural colors arising from periodic nanostructures, which show great potential value for fundamental research and practical applications. Here, a novel cellular mechanical visualizable biosensor formed by assembling engineered cardiac tissues on the *Morpho* butterfly wings is presented. The assembled cardiomyocytes benefit from the periodic parallel nanoridges of the wings and can recover their autonomic beating ability with guided cellular orientation and good contraction performance. As the beating processes are accompanied by the cardiomyocytes' elongation and contraction, the elastic butterfly wing substrate undergoes the same cycle of deformations, which causes corresponding synchronous shifts in their structural colors and photonic bandgaps for self-reporting of the cell mechanics. It is demonstrated that this self-reporting performance can be further improved by adding oriented carbon nanotubes in the nanoridges of the wings for the culture. In addition, taking advantage of the similar size of the cardiomyocyte and a single *Morpho* wing scale, the investigation of single-cell-level mechanics can be realized by detecting the optical performance of a single scale. These remarkable properties make these butterfly wings ideal platforms for biomedical research.**

Morpho butterflies have parallel, periodic nanoridges on the surfaces of their wing scales, which can control the propagation of photons in their photonic bandgap (PBG).[1–5] This gives these wings brilliant structural colors and makes them important in bionics. Marveling at this elaborate architecture, researchers have carefully studied the bionic manufacture and applications of butterfly scales.[6–18] Many functional objects with surface morphologies similar to the butterfly scales have been developed using nanotechnologies in photonic devices, sensors, self-cleaning surfaces, liquid condensers, and so on.[19–27] Although these bionic attempts have new functionalities and visual effects, the exact combination of the cuticle complex refractive index and subtle 3D structures of the butterfly scales are still beyond current nanofabrication capacities. In addition, because of the limited commonality between biological and engineering solutions, some important biomedical values of these butterflies remain unexplored.

Here, we show that by assembling engineered cardiomyocyte tissues on the *Morpho* butterfly wings, a novel biological sensor with the feature of cellular mechanical visuals can be constructed, as indicated in **Figure 1**. We found that the parallel periodic nanoridges of the butterfly wings could effectively promote the assembled cardiomyocytes to recover their autonomic beating ability with guided cellular orientation and improved contraction performance on their surfaces. As the beating processes are accompanied by the cardiomyocytes' elongation and contraction,[28–34] the elastic butterfly wing substrate will undergo the same cycle of deformations, causing corresponding synchronous shifts in their structural colors and PBGs to offer self-reporting of the cell mechanics. In addition, with the oriented filling of carbon nanotubes in the gaps between these nanoridges, the self-reporting performance of the cardiomyocytes on the butterfly wings could be further improved because of the enhanced beating consistency of cardiomyocytes on the conductive substrates and the increased contrast of the structural colors on the black background. More attractively, because of the similar dimensions of the cardiomyocyte and a butterfly scale, the investigation of single-cell-level mechanics could be realized by detecting the optical performance of a single scale. Thus, natural creatures, such as the *Morpho* butterfly, are valuable for biomedical applications.

In a typical experiment, the wings of *Morpho Menelaus* (*M. Menelaus*) were used for cell culture and sensor construction. *M. Menelaus* is one of the tropical *Morpho* butterflies. On the wing of mature *M. Menelaus*, the shape and the size of these two scales are relatively uniform, which are rectangular with the length-width ratio of 2.1 to the ground scale and 2.99 to the cover scale (Table S1, Supporting Information). Its wing surface is made up of two kinds of scale, "ground" and "glass" scales, which are highly ordered and arranged like tiles. The ground scales are the basis of the structural color, while the transparent glass scales situated above the ground scales exhibit relatively low structural color (Figure S1, Supporting Information). The scales are composed of periodic parallel cuticle ridges, and a single ridge consists of a stack of alternating chitin and air multilayered lamellae, which is called a "Christmas-tree" structure. This elaborate structure is the foundation of the bright structural color of *M. Menelaus*' wings. Because of the multilayer interference caused by the ridge lamellae hierarchical structure, the *M. Menelaus* wing possesses the unique PBG property of wavelength selective capability. When certain light wavelengths illuminate the PBG, they are prevented from propagating through the wing and are reflected back. Considering the

Dr. Z. Y. Chen, Dr. F. F. Fu, Dr. Y. R. Yu, Dr. H. Wang, Dr. Y. X. Shang, Prof. Y. J. Zhao
State Key Laboratory of Bioelectronics
School of Biological Science and Medical Engineering
Southeast University
Nanjing 210096, China
E-mail: yjzhao@seu.edu.cn

DOI: 10.1002/adma.201805431

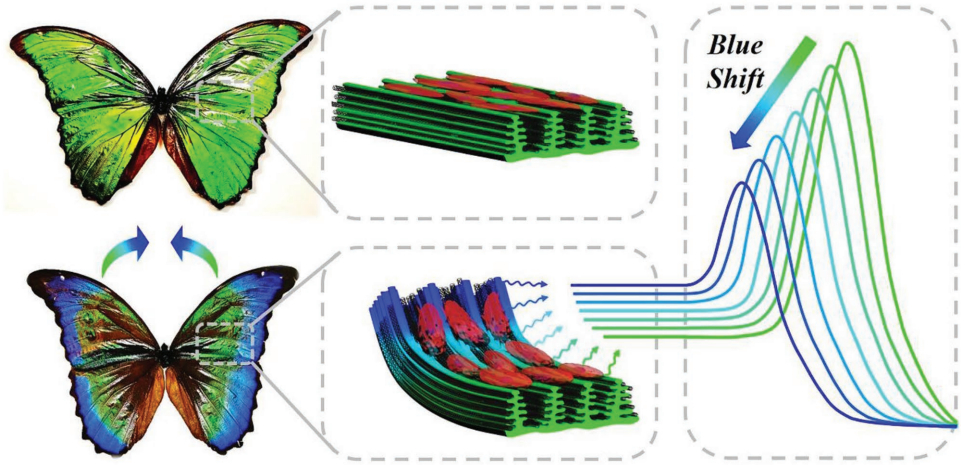

Figure 1. Scheme of the construction of the visualized detection platform by assembling engineered cardiomyocytes on the modified *Morpho* wings.

"Christmas-tree" structure as multilayer horizontal model layers, the reflection peak position λ of *M. Menelaus* wings can be estimated as

$$\frac{k^2}{4d^2}\lambda^2 = n_e^2 - \sin^2 i \quad (1)$$

where d is the equivalent thickness of the multilayer structure, n_e is the effective refractive index, k is an integer, and i is the incident angle.[35] Normally, d is nearly constant and n_e is relatively constant in a certain medium, and the value of λ mainly depends on i. Thus, with the incident angle increasing at the direction parallel to the long axis of the scale multilayers, the reflection peak decreases, showing a blueshift. However, due to the lacking of the ordered nanostructures among these "Christmas-tree" ridges, there is unobvious angle-dependency at the direction perpendicular to the long axis (Figure S2, Supporting Information). Therefore, when observed at the parallel direction to the long axis of scale, the color of the *M. Menelaus* wing changes synchronously under different viewing angles. This implies that when the *M. Menelaus* wing is deformed, the changes of concurrent structural color could be employed for self-reported mechanical sensing.

It is worth mentioning that although current nanotechnologies had made progress to achieve the goal to construct such elaborate and complex structures,[36] it would be fairly expensive and time consuming. With the highly cost and photoresist materials limitations, the artificial butterfly wing-like photonic structures could not be manufactured in large and could not be considered as the cardiac sensing materials. In addition, the *M. Menelaus* wing was also used as template to acquire replications with desired biocompatible materials on the consideration of further cell culture. It was found that soft hydrogel could hardly remain the precise photonic structures; while for hard hydrogel, the wing scale kept inlaid and the replica was too stiff to generate elastic changes when cultured with cardiomyocytes (Figure S3, Supporting Information). Taking all the factors into consideration, the natural structured *M. Menelaus* wing would be an optimal choice with whose surface properties and biocompatibility could be improved by chemical processing methods.

To improve the *M. Menelaus* wings' capacity for cell culture and self-reported sensing, their surfaces were modified, as shown in **Figure 2**a. The wings were first treated by oxygen plasma to gain hydrophilic surface wettability from the highly hydrophobic original. The thickness of chitin lamellae on the *M. Menelaus* wing was slightly decreased by the high-energy plasma beam. In this step, although some neighboring ridges on the scales showed partial discontinuous conglutination, the primary nanomorphology of the surface of the scales was retained, and the overturned cross scale section also showed parallel nanostructure (Figure 2b,c). As d decreased, the reflection position shifted slightly toward blue (Figure S4, Supporting Information). Because of the parallel ridges, carbon nanotubes could be orientated to fill the gaps between the nanoridges by slowly pulling the wing up from a carbon nanotube solution (Figure 2d,e). With the carbon nanotubes' integration, the parameter n_e in Equation (1) increased, causing a redshift of the *M. Menelaus* wing's reflection wavelength. Surprisingly, we found that the contrast of the structural color increased after carbon nanotube filling, as the nanotubes provided a black background (Figure S4, Supporting Information). Finally, to obtain better biocompatibility and nutritional capacity, bioactive methacrylated gelatin (GelMA) hydrogel was used for further filling of the interspace among the carbon nanotubes and ridges, connecting them with the hydrogel network structure. The hydrogel also formed a thin layer covering the scales' surface (Figure 2f,g).

To further confirm the colorimetric mechanical sensing capability of the *M. Menelaus* wings, their mechanical strength, integrity, resistance, and optical consistency and reproducibility were tested. It was found that the *M. Menelaus* wings were with sensitive mechanical responses (Figure S5, Supporting Information) and showed good integrity and resistance during several bending cycles. In addition, although with some modification processes, the optical variability in the *M. Menelaus* wing scales was negligible, with the variable coefficients around 0.42% (Figure S6, Supporting Information).

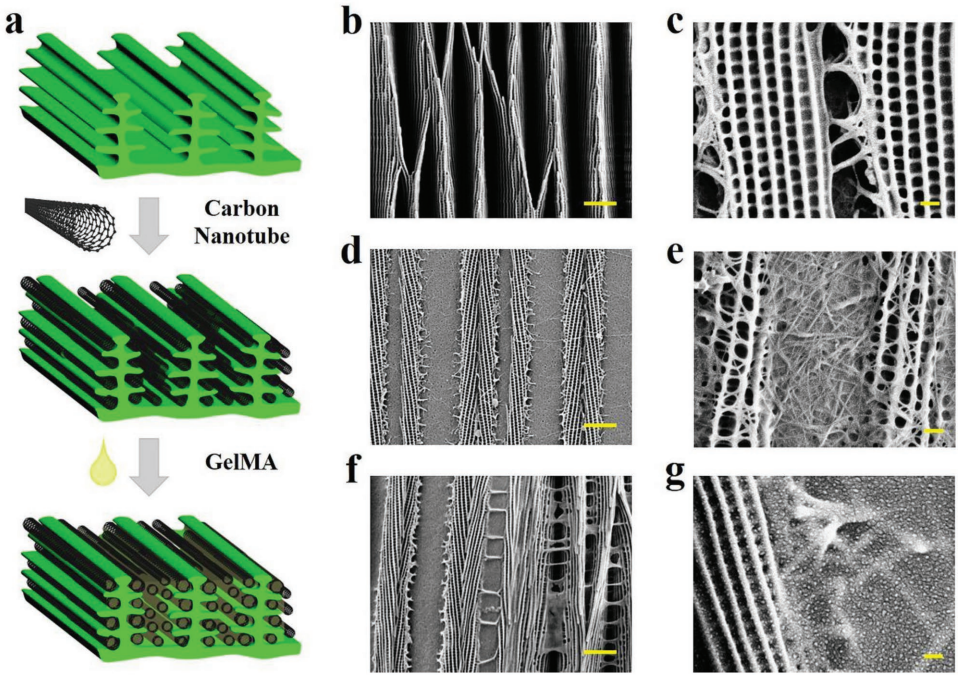

Figure 2. Scheme and SEM images of modification. a) Scheme of the modification process on *M. Menelaus* wing. b) SEM image of the scale after oxygen plasma treatment. c) Magnifying SEM image of the cross section of ridges. d) SEM image of the scale with self-assembled carbon nanotubes. e) Magnifying image of carbon nanotubes in (d). f) SEM image of the scale covered by GelMA hydrogel. g) Magnifying image of GelMA hydrogel cover. The scale bars are 2 µm in (b,d,f) and 200 nm in (c,e,g).

To investigate their biological value, the modified *M. Menelaus* wings were used as a substrate for the culture of neonatal rat ventricular cardiomyocytes. We found that cardiomyocytes were oriented randomly in general plate culture, while most cardiac cells cultured on the modified *M. Menelaus* wing showed marvelous concurrent orientation (**Figure 3** and Figure S7, Supporting Information). The main reason is the specific stripe nanostructure of the *M. Menelaus* wing surface.

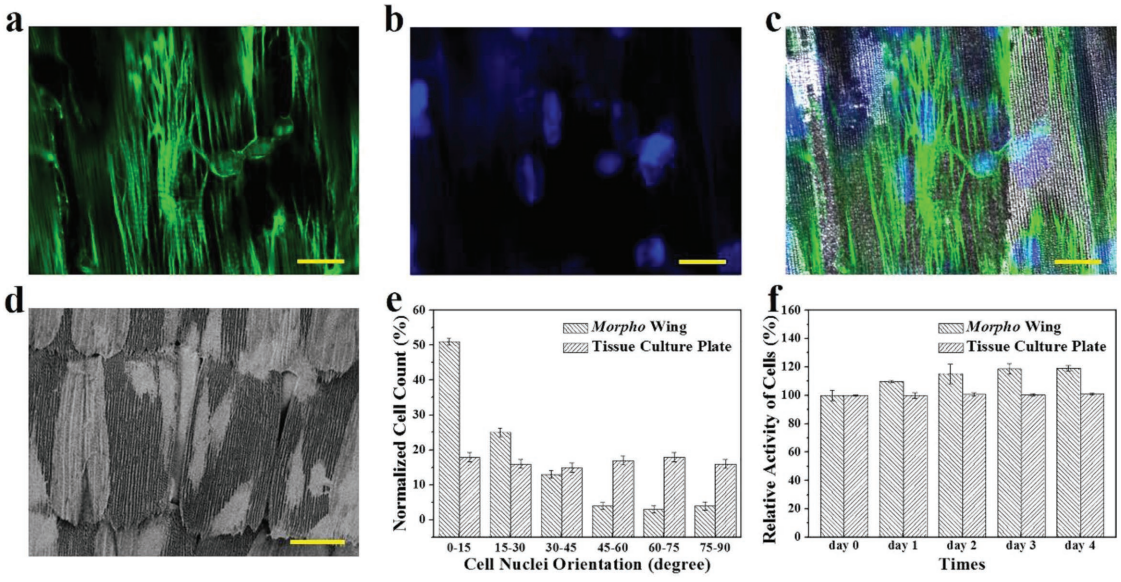

Figure 3. Cardiomyocytes cultured on modified *M. Menelaus* wing scales. a–c) Fluorescence images of the cardiomyocytes cultured on the modified *M. Menelaus* wing scales for: a) F-actin, b) nuclei, and c) the merged field, respectively. d) SEM images of cardiomyocytes cultured on the modified *M. Menelaus* wing scales. e) Orientation angle frequency distribution of the cardiomyocytes on the *M. Menelaus* wing and tissue culture plate. f) MTT cell activity array [by 3-(4, 5,-dimethyl-2-thiazolyl)-2, 5-diphenyl-2-H-tetrazolium bromide (MTT)] between cardiomyocytes cultured on the modified *M. Menelaus* wing and cell plate. The bars are 10 µm in (a–c) and 100 µm in (d).

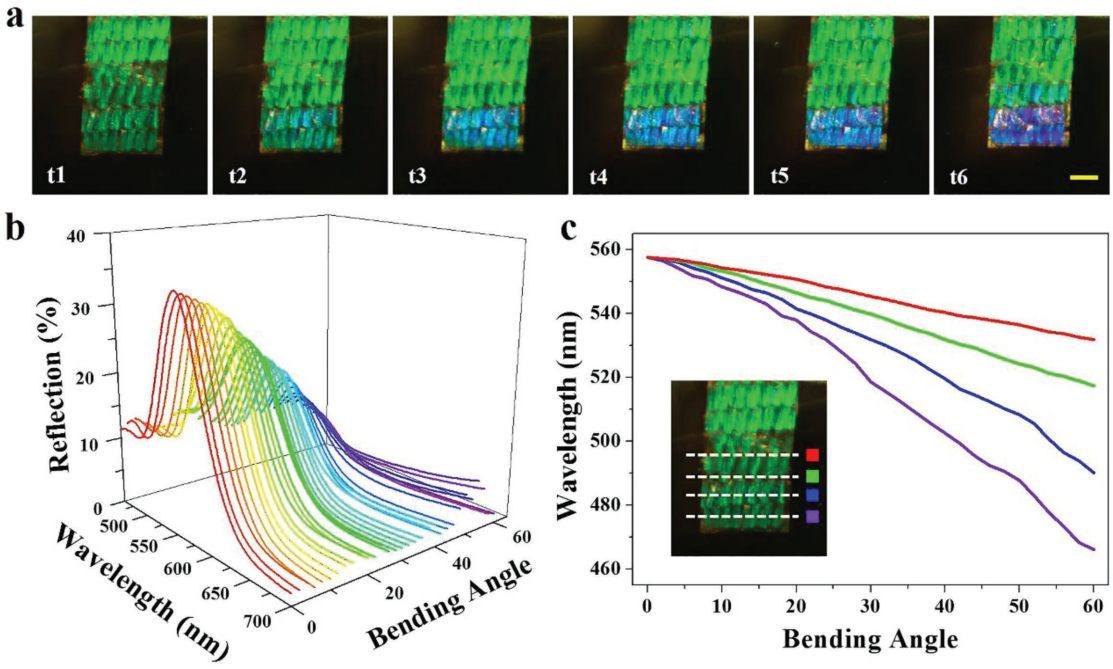

Figure 4. The color changing process of *M. Menelaus* butterfly wings actuated by cardiomyocytes. a) Optical microscopy images of the structural color variation process of the cardiomyocytes cultured *M. Menelaus* wing during half myocardial cycles (from t1 to t6). b) Dynamic reflectance wavelengths of the *M. Menelaus* wing during half myocardial cycles at the position of the wing's outer edge. c) Relationship between the bending angles of the *M. Menelaus* wing and the reflection peak values in different positions of the rectangle-shaped wing.

With the parallel nanoridges, the cultured cardiomyocytes tended to be induced into alignment and elongated along the ridges. Taking advantage of phalloidin and 4′,6-diamidino-2-phenylindole (DAPI) staining, the sarcomere formation, the directions of induced cardiomyocyte cell orientation, and elongated cell nuclei were much more obvious on the modified *M. Menelaus* wing. These cardiomyocytes grew along the direction of the parallel ridges, and the nonrandom sarcomere alignment, cardiomyocyte nuclei, and ridges of the wing scale were more apparent in enlarged views (Figure 3a–c). This was further confirmed by using immunostaining for cardiac troponin T (cTnT), which also showed the induced orientation of the cardiomyocytes (Figure S8, Supporting Information). These cultured cardiomyocytes also exhibited induced orientation with distinct cell bipolarizations along the ridges in scanning electron microscopy (SEM) images (Figure 3d). These indicated that the modified *M. Menelaus* wing could provide 3D growth space for cardiomyocytes and could mimic a tissue scaffold.

As further confirmation of the major trend, the angles between the growth direction of the cardiomyocytes and the parallel ridges were measured and analyzed (Figure 3e). The results demonstrated that about 76% of the cardiomyocytes on the *M. Menelaus* wing showed an orientation within 30° of the ridges' direction, while cardiomyocytes cultured on plates displayed no particular orientation. A cell activity array was also employed to compare the cultured cell activity between the modified *M. Menelaus* wing and a plate (Figure 3f). We found that cell activity of living cardiomyocytes assembled on wing slight better than plate's, which indicated that the modified wing possessed strong biocompatibility and great biomedical value for cell adhesion and alignment.

The assembled cardiomyocytes recovered their stable beating after culturing on modified *M. Menelaus* wing for 2 d. Because of the flexibility of the *M. Menelaus* wing, the beating of the cardiomyocytes caused the wing to bend during contraction and to return to its original shape during relaxation. During these rhythmic beating cycles, the *M. Menelaus* wing was changed reversibly from a fixed vertical observation position (**Figure 4**a). As the *M. Menelaus* wing's actuated bending range increased, the normal line of the wing slanted gradually, which caused the angle between the vertical observing direction and the normal line to increase accordingly. According to Equation (1) and the definition of the incident angle, i was continuously rising and the reflection wavelength λ decreased accordingly when the cardiomyocytes' contractions caused the *M. Menelaus* wing to move like a live butterfly's flapping wings. As the *M. Menelaus* wing flapped, the structural color of the wing's outer edge first transited from green to blue, then spread gradually inside the wing with decreased color transition.

The relationship between the shifted structural colors and the bending angles was investigated. Different positions from the *M. Menelaus* wing were chosen to record the variations in characteristic reflection peak positions (Figure 4b,c). For each position at different bending angles, the *M. Menelaus* wing had the corresponding structural colors. Thus, the evaluation of cardiomyocyte contraction could be observed from the changes of *M. Menelaus* wing's structural color with the naked eye and could also be estimated by quantitative spectrometric analysis. It should be mentioned that both the contraction ability and the frequency of cardiomyocytes cultured on the *M. Menelaus* wing with carbon nanotubes were higher than wings without the

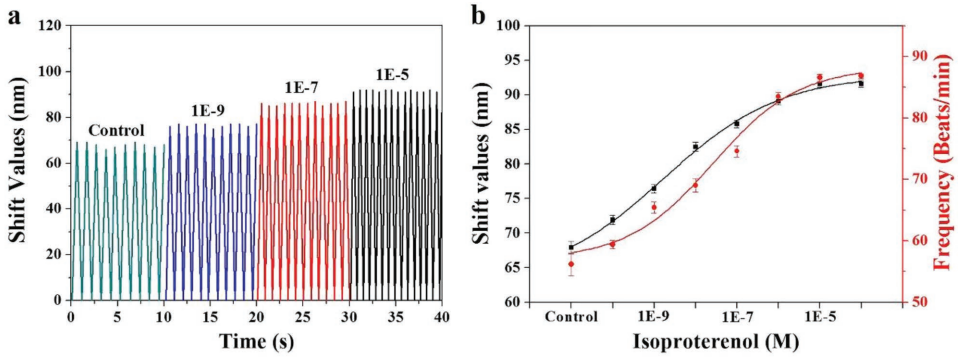

Figure 5. The application of cardiac cultured *M. Menelaus* wing as a drug evaluation platform. a) Relationship between the reflection peak shift values and the beating speed of the *M. Menelaus* wing at the same outer edge mentioned in Figure 4b. b) The relationships of the average peak shift values (black) and the beating frequency (red) to the bend up process of the *M. Menelaus* wing with different isoproterenol concentration.

nanotubes (Movies S1 and S2, Supporting Information). This is presumably because the carbon nanotubes enhanced the beating consistency of the cardiomyocytes on the conductive substrates and increased the contrast between the structural colors and the black substrate. These results indicated that the modified *M. Menelaus* wing had good self-reporting capability of the cardiomyocytes' contraction performance and biosensing functionality. It was worth mentioning that not only the neonatal rat cardiomyocytes but also cardiomyocyte cells derived from induced pluripotent stem cell (iPS cell) could be employed to actuate the sensing substrate. However, compared to the primary cell, the iPS derived cardiomyocyte cells only showed the weakened driving force, which needed further optimization (Figure S9, Supporting Information).

To explore their potential value, the *M. Menelaus* butterfly wings driven by neonatal rat cardiomyocytes were employed as a drug evaluation platform. As a typical test, isoproterenol at various concentrations was added to the cardiac culture medium and used to stimulate the cardiomyocytes. In the control group of normal cultural condition, the structural color of the outer edge of the *M. Menelaus* wing was changed from green to blue (as mentioned above), and the reflection peak shifted from 558 to 483 nm. However, the structural color at the same place on the wing changed to dark blue, and the reflection peak blueshifted to 470 nm with the addition of 1×10^{-6} M isoproterenol in the culture medium (Movie S3, Supporting Information). We found that the degree of structural color changes and the blueshift values of the characteristic reflection peaks of the *M. Menelaus* wing increased with the increased isoproterenol concentration (**Figure 5**a). The addition of the isoproterenol also affected the beat frequency of the cardiomyocytes. A positive chronotropic response was observed by increasing the concentration of the isoproterenol (Figure 5b and Figure S10, Supporting Information), which indicated that the biological effect of isoproterenol on the *M. Menelaus* wing persisted in vivo, exhibiting increased beat frequency. Hence, the *M. Menelaus* wing platform exhibited excellent self-reporting performance and prospects for application for visual drug screening, examining, and evaluating.

Because of the similar size of cardiomyocytes and the *M. Menelaus* wing scales, detection at the level of a single cell could be constructed based on this platform by analyzing the optical performance of a single scale (**Figure 6**a). For this purpose, the transparent glass scales with their different structural color intensities were all removed from the base, and most of the ground scales were also stripped to build single-scale platforms. Other modification steps for the residual scales were generally the same as those in the previous *M. Menelaus* wing treatment process. After cardiomyocyte culture, we found that a single scale with a size of around 90 μm × 150 μm could support the growth of just a few cells. The cardiomyocytes cultured on the single scale also exhibited obvious alignment and elongation (Figure 6b–e). When these cardiomyocytes recovered their beating cycles, they could actuate a single scale so that it rotated rhythmically along the short edge joining the wing substrate. As the single scale rotated, the structural color of the whole scale transited from green to blue, as shown in Figure 6f–k and Movie S4 in Supporting Information. In contrast to existing single-cell-level monitoring with complex instruments and strategies,[37,38] the beating frequency and contractility of the cultured cardiomyocytes could be observed and evaluated by the naked eye or simple spectrum analysis. Thus, the *M. Menelaus* wing could be developed into a single-cell-level detecting and monitoring platform for biological research and drug screening.

In summary, we have developed a cellular, visualizable biosensor by assembling cardiomyocytes on *Morpho* wings. Because of the periodic nanoridges on the wing scales, the cultured cardiomyocytes could be assembled in an induced orientation and could recover their autonomic beating. As the cardiomyocytes contracted and elongated during their beating cycles, the flexible wing was driven to deform correspondingly, causing synchronous reflection wavelength shifts that allowed visual sensing of cell mechanics. We found that this self-reporting performance could be improved by filling the gaps between the nanoridges of the wing with carbon nanotubes, which contributed to better cardiomyocyte cooperativity and consistency because of the nanotubes' conductivity and the greater structural color contrast provided by the dark background. A single-cell-level mechanics platform could be constructed by culturing the cardiomyocytes on a single scale and detecting its optical shifts.

The combination of carbon-nanotube-integrated *M. Menelaus* wing and assembled cardiomyocyte tissues offered a flexible and self-reporting substrate and improved cell-induced

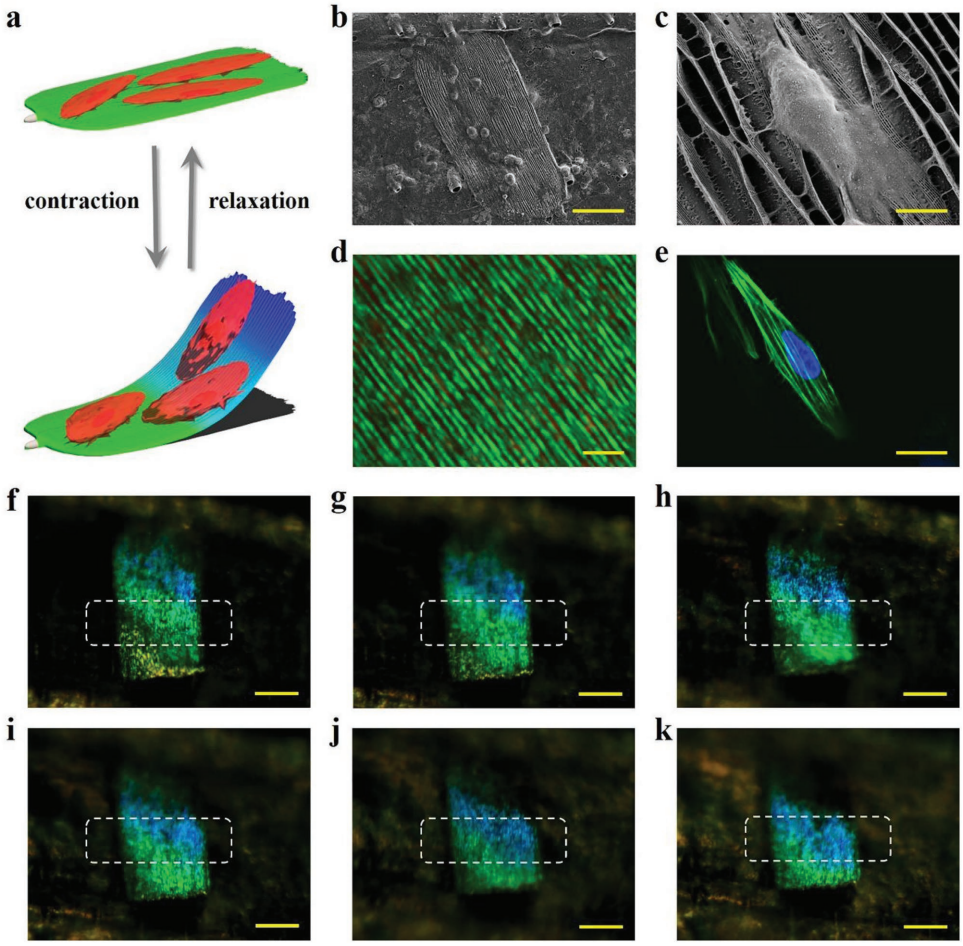

Figure 6. A single-cell-level detection platform constructed by single *M. Menelaus* wing scale. a) Scheme of the single wing scale for single-cell-level detection. b) SEM images of the single scale with cardiomyocytes. c) Magnifying SEM image of the cardiomyocyte on the single scale. d) Optical image of culture medium infiltrated *M. Menelaus* wing scale. e) Fluorescence image of the single cardiomyocyte on the single wing scale for the merged field of F-actin and nuclei. F–k) Optical microscopy images of the structural color variation process of the single wing scales during half myocardial cycles. The bars are 50 μm in (b,f–k), and 5 μm in (c–e).

orientation and cooperation, which provide a novel platform for cardiac culture. As the *M. Menelaus* wing is a natural creation, the substrate materials are easy to obtain without complex fabrication and preparation. When the cardiomyocytes cultured on the *M. Menelaus* wing recover their autonomic circulatory contraction and elongation beating process, their mechanics can be measured and analyzed by simple optical sensing, avoiding the expenditure and complexity of large instruments and detecting methods. More importantly, single-cell-level detection is gaining increasing significance in current research, but existing measurements mainly depend on composite living-cell analysis systems including high-definition imaging devices and staining of living cells. In contrast, with our present platform based on *M. Menelaus* wing scales, the estimation of a single cardiomyocyte's mechanical performance only requires a spectrograph and spectral analysis, which is a simple, low-cost operation. Thus, we believe that our method of culturing cardiomyocytes on *Morpho* wings possesses huge potential in biological research and drug development.

Supporting Information

Supporting Information is available from the Wiley Online Library or from the author.

Acknowledgements

This work was supported by the National Key Research and Development Program of China (2017YFA0700404), the National Science Foundation of China (Grant Nos. 21473029 and 51522302), the NSAF Foundation of China (Grant No. U1530260), the Scientific Research Foundation of Southeast University, and the Scientific Research Foundation of Graduate School of Southeast University. All animal experiments were approved by the Animal Ethics Committee of Southeast University (No. 20180326003) and were conducted in compliance with the Regulations for the Administration of Affairs Concerning Experimental Animals of China.

Conflict of Interest

The authors declare no conflict of interest.

Keywords

carbon nanotubes, cardiomyocytes, heart on a chip, *Morpho* butterflies, structural color

Received: August 20, 2018
Revised: November 25, 2018
Published online:

[1] P. Vukusic, J. R. Sambles, *Nature* **2003**, *424*, 852.
[2] S. Kinoshita, S. Yoshioka, J. Miyazaki, *Rep. Prog. Phys.* **2008**, *71*, 076401.
[3] O. Sato, S. Kubo, Z. Z. Gu, *Acc. Chem. Res.* **2009**, *42*, 1.
[4] H. Butt, A. K. Yetisen, D. Mistry, S. A. Khan, M. U. Hassan, S. H. Yun, *Adv. Opt. Mater.* **2016**, *4*, 497.
[5] M. A. Giraldo, S. Yoshioka, C. Liu, D. Stavenga, *J. Exp. Biol.* **2016**, *219*, 3936.
[6] J. X. Wang, Y. Z. Zhang, S. T. Wang, Y. L. Song, L. Jiang, *Acc. Chem. Res.* **2011**, *44*, 405.
[7] F. F. Fu, Z. Y. Chen, Z. Zhao, H. Wang, L. R. Shang, Z. Z. Gu, Y. J. Zhao, *Proc. Natl. Acad. Sci. USA* **2017**, *114*, 5900.
[8] Y. D. Liu, J. Goebl, Y. D. Yin, *Chem. Soc. Rev.* **2013**, *42*, 2610.
[9] J. Wang, L. Y. Sun, M. H. Zou, W. Gao, C. H. Liu, L. R. Shang, Z. Z. Gu, Y. J. Zhao, *Sci. Adv.* **2017**, *3*, e1700004.
[10] T. S. Shim, S. H. Kim, J. Y. Sim, J. M. Lim, S. M. Yang, *Adv. Mater.* **2010**, *22*, 4494.
[11] Z. W. Mao, H. L. Xu, D. Y. Wang, *Adv. Funct. Mater.* **2010**, *20*, 1053.
[12] J. Wang, M. H. Zou, L. Y. Sun, Y. Cheng, L. R. Shang, F. F. Fu, Y. J. Zhao, *Sci. China Mater.* **2017**, *60*, 857.
[13] A. G. Dumanli, T. Savin, *Chem. Soc. Rev.* **2016**, *45*, 6698.
[14] M. X. Kuang, J. X. Wang, L. Jiang, *Chem. Soc. Rev.* **2016**, *45*, 6833.
[15] C. H. Liu, H. B. Ding, Z. Q. Wu, B. B. Gao, F. F. Fu, L. R. Shang, Z. Z. Gu, Y. J. Zhao, *Adv. Funct. Mater.* **2016**, *26*, 7937.
[16] S. H. Kim, H. S. Park, J. H. Choi, J. W. Shim, S. M. Yang, *Adv. Mater.* **2010**, *22*, 946.
[17] J. P. Ge, Y. D. Yin, *Angew. Chem., Int. Ed.* **2011**, *50*, 1492.
[18] F. F. Fu, L. R. Shang, F. Y. Zheng, Z. Y. Chen, H. Wang, J. Wang, Z. Z. Gu, Y. J. Zhao, *ACS Appl. Mater. Interfaces* **2016**, *8*, 13840.
[19] R. A. Potyrailo, H. Ghiradella, A. Vertiatchikh, K. Dovidenko, J. R. Cournoyer, E. Olson, *Nat. Photonics* **2007**, *1*, 123.
[20] R. A. Potyrailo, *Chem. Soc. Rev.* **2017**, *46*, 5311.
[21] A. D. Pris, Y. Utturkar, C. Surman, W. G. Morris, A. Vert, S. Zalyubovskiy, T. Deng, H. T. Ghiradella, R. A. Potyrailo, *Nat. Photonics* **2012**, *6*, 195.
[22] F. Y. Zhang, Q. C. Shen, X. D. Shi, S. P. Li, W. L. Wang, Z. Luo, G. F. He, P. Zhang, P. Tao, C. Y. Song, W. Zhang, D. Zhang, T. Deng, W. Shang, *Adv. Mater.* **2015**, *27*, 1077.
[23] M. Y. Cao, X. Jin, Y. Peng, C. M. Yu, K. Li, K. S. Liu, L. Jiang, *Adv. Mater.* **2017**, *29*, 1606869.
[24] S. Huang, D. Y. Wang, *Angew. Chem., Int. Ed.* **2017**, *56*, 9053.
[25] X. Yao, Y. L. Song, L. Jiang, *Adv. Mater.* **2011**, *23*, 719.
[26] C. C. Liu, J. Ju, Y. M. Zheng, L. Jiang, *ACS Nano* **2014**, *8*, 1321.
[27] Q. C. Shen, J. Q. He, M. T. Ni, C. Y. Song, L. Y. Zhou, H. Hu, R. X. Zhang, Z. Luo, G. Wang, P. Tao, T. Deng, W. Shang, *Small* **2015**, *11*, 5705.
[28] A. W. Feinberg, A. Feigel, S. S. Shevkoplyas, S. Sheehy, G. M. Whitesides, K. K. Parker, *Science* **2007**, *317*, 1366.
[29] F. F. Fu, L. R. Shang, Z. Y. Chen, Y. R. Yu, Y. J. Zhao, *Sci. Rob.* **2018**, *3*, eaar8580.
[30] S. R. Shin, R. Farzad, A. Tamayol, V. Manoharan, P. Mostafalu, Y. S. Zhang, M. Akbari, S. M. Jung, D. Kim, M. Comotto, N. Annabi, F. E. Al-Hazmi, M. R. Dokmeci, A. Khademhosseini, *Adv. Mater.* **2016**, *28*, 3280.
[31] A. J. Ryan, C. J. Kearney, N. Shen, U. Khan, A. G. Kelly, C. Probst, E. Brauchle, S. Biccai, C. D. Garciarena, V. Vega-Mayoral, P. Loskill, S. W. Kerrigan, D. J. Kelly, K. Schenke-Layland, J. N. Coleman, F. J. O'Brien, *Adv. Mater.* **2018**, *30*, 1706442.
[32] S. R. Shin, C. Zihlmann, M. Akbari, P. Assawes, L. Cheung, K. Z. Zhang, V. Manoharan, Y. S. Zhang, M. Yuksekkaya, K. T. Wan, M. Nikkhah, M. R. Dokmeci, X. W. Tang, A. Khademhosseini, *Small* **2016**, *12*, 3677.
[33] Y. R. Yu, F. F. Fu, L. R. Shang, Y. Cheng, Z. Z. Gu, Y. J. Zhao, *Adv. Mater.* **2017**, *29*, 1605765.
[34] J. U. Lind, T. A. Busbee, A. D. Valentine, F. S. Pasqualini, H. Y. Yuan, M. Yadid, S. J. Park, A. Kotikian, A. P. Nesmith, P. H. Campbell, J. J. Vlassak, J. A. Lewis, K. K. Parker, *Nat. Mater.* **2017**, *16*, 303.
[35] S. Berthier, E. Charron, A. Da Silva, *Opt. Commun.* **2003**, *228*, 349.
[36] X. J. Liu, H. C. Gu, M. Wang, X. Du, B. B. Gao, A. Elbaz, L. D. Sun, J. L. Liao, P. F. Xiao, Z. Z. Gu, *Adv. Mater.* **2018**, *30*, 1800103.
[37] E. H. Kim, G. Chin, G. X. Rong, K. E. Poskanzer, H. A. Clark, *Acc. Chem. Res.* **2018**, *51*, 1023.
[38] T. E. Lin, S. Rapino, H. H. Girault, A. Lesch, *Chem. Sci.* **2018**, *9*, 4546.